



Solubility of Sb in binary Na₂CO₃–NaCl molten salt

Yong-ming CHEN¹, Long-gang YE¹, Chao-bo TANG¹, Sheng-hai YANG¹, Mo-tang TANG¹, Wen-hai ZHANG^{1,2}

1. School of Metallurgy and Environment, Central South University, Changsha 410083, China;

2. China Nerin Engineering Co., Ltd., Nanchang 330031, China

Received 27 October 2014; accepted 20 January 2015

Abstract: The interaction between molten Na₂CO₃–NaCl salt and Sb and the solubility of Sb in molten salt were investigated in the temperature range of 700–1000 °C. The results show that the dissolution equilibrium of Sb in molten salt can be achieved in 3 h, and the amount of Sb dissolved in the melt decreases as the viscosity decreases. The solubility limits in an eutectic mixture were determined as 5.42%, 2.42%, 0.75% and 0.68% at 700, 800, 900 and 1000 °C, respectively. A high temperature and appropriate content of NaCl will decrease the dissolution of Sb. The insoluble Sb was collected at the bottom of molten salt. The Sb dissolved on the surface of the molten salt is easily oxidized, whereas the Sb dissolved inside the molten salt is randomly distributed in terms of the form of metal Sb.

Key words: Sb; solubility; molten salt; viscosity

1 Introduction

Molten salts are used in materials preparation [1,2], solar power plants [3–5] and other engineering fields [6–8]. As the simplest binary system, eutectic Na₂CO₃–NaCl molten salts have been widely used as the solvents in quenching baths for steel [9,10], ceramic-materials preparation [11], municipal-waste disposition [7] and other engineering processes. Recently, molten alkali and chloride salts (Na₂CO₃, Na₂CO₃–NaCl, K₂CO₃–KCl) have also been used for stibnite and bismuth glance ore smelting [12,13] to replace the traditional ternary slag of FeO–SiO₂–CaO in traditional antimony smelting process. This new process used molten salt as an inert reaction medium; Sb₂S₃ was reduced to the metal by carbothermic and desulfurization reactions and gathered at the bottom of the molten salt after being extracted by natural sedimentation. The significant reduction of the smelting temperature will result in an obvious decrease in energy consumption, at the same time, which provides the outstanding advantages of eliminating SO₂ discharge while utilising the larger zinc ash resources.

Although the use of molten Na₂CO₃–NaCl to extract Sb from stibnite is a cleaning process, the data on

the dissolution behaviors and the solubility limit of Sb in binary Na₂CO₃–NaCl systems are still scarce. A high solubility of Sb in molten salt will increase the mechanical loss during the smelting process and decrease the recovery rate of Sb. In the present study, the dissolution behaviors including solubility of Sb in salt and interaction between Na₂CO₃–NaCl melt and Sb were investigated in the 700–1000 °C temperature range. The research results have a significant guidance on the molten salt smelting of Sb, and it also can promote the new process development of other heavy metals.

2 Experimental

The Na₂CO₃ and NaCl used in this experiment were analytical grade (99%) and were dried in an oven at 270 °C for 24 h. The antimony used was high purity (99.99%). As the phase diagram in Factsage shows, the eutectic temperature is 635 °C for the composition of $n(\text{Na}_2\text{CO}_3)/[n(\text{Na}_2\text{CO}_3)+n(\text{NaCl})]=0.423$, where n represents the amount of substance. The Na₂CO₃ and NaCl were charged into a corundum crucible (diameter 3 cm, height 5 cm) in the necessary proportion and heated to melt completely. Next, the metal was submerged into the melt, and this moment was defined as the experiment start time. Approximately 5 g and 1 g of

the salt and metal sample, respectively, were used each time. All experiments were carried out with dehydrated high-purity argon gas. After the predetermined experimental time, the sample was quenched by flushing argon gas. The metal and flux were separated for chemical analysis. Inductively coupled plasma atomic emission spectroscopy was used to analyze the content of Sb in the solid salt.

Viscosity measurements were performed using a RTW-10 instrument for testing melt physical properties (Kexiang Instrument Co., Ltd., Anshan, China). This measurement system included an electric furnace with a temperature-controlling program, sensors, a computer equipped with test software and a holder. The viscosities of the binary $\text{Na}_2\text{CO}_3\text{-NaCl}$ samples were measured by the horizontal-hammer method. After heat treatment, the specimens were examined by an ESCALAB Mark II X-ray photoelectron spectrometer (VG scientific, UK). The XPS spectrometer consisted of an X-ray source, which was Al K_α radiation in ultra-high vacuum (3.56×10^{-5} Pa). The C 1s peak (284.8 eV) was used as the internal standard for binding-energy calibration. X-ray diffraction (XRD) studies were performed using Rigaku D/max 2550VB+18 kW powder diffractometer with a Cu K_α X-ray source at 40 kV and 300 mA. To investigate the diffusion homogenization of Sb in molten salt, the saturation salt was quenched to room temperature, and the block sample was cut along the diameter to obtain a flat cross-section. The distribution of Sb along the diameter was monitored by a JEOL JSM-6360LV scanning electron microscope (SEM) coupled with an X-ray electron dispersive spectroscope (EDS).

3 Results and discussion

3.1 Solubility in eutectic system

The $\text{Na}_2\text{CO}_3\text{-NaCl}$ binary system has an eutectic point of 635 °C. A reduction in the melting point decreases the operation temperature. The solubility of Sb in eutectic molten salt as a function of time and temperature is presented in Fig. 1. It can be seen from the figure that both temperature and time have a strong influence on the solubility of Sb. The dissolution of Sb achieved equilibration quickly, and the time needed to reach equilibrium is related to temperature. The equilibration time was found to be 3 h at 800 °C; however, at 700 °C, there was a slow increase after 3 h. Due to the acceleration of ionic migration and molecular diffusion at high temperature, the dissolution equilibration was achieved quickly. The solubility of Sb has a small increase with time increasing, which was caused by the volatilization of molten salt [14], so the relative content of Sb was increased.

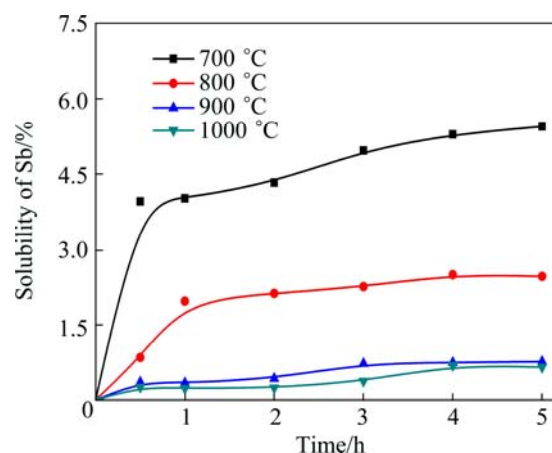


Fig. 1 Solubility of Sb at different temperatures and time in eutectic $\text{Na}_2\text{CO}_3\text{-NaCl}$ molten salt

However, the solubility of Sb in molten $\text{Na}_2\text{CO}_3\text{-NaCl}$ decreases as the temperature increases, in contrast to the dissolution of other compounds in molten salt. After 3 h, the dissolution reached 4.9741%, 2.2709%, 0.7298% and 0.3763% at 700, 800, 900 and 1000 °C, respectively. The melting point is 635 °C, although the molten salt was an eutectic mixture. Thus, the viscosity of the flux was high at temperatures greater than but relatively close to the melting point, and the viscosity decreased obviously as the temperature increased. As the temperature increased from 700 °C to 1000 °C, the viscosity decreased from 17.0213 mPa·s to 0.9063 mPa·s. This can be explained by the decrease in the solubility of Sb as the temperature increases. As shown in Fig. 2, both the solubility of Sb and the viscosity of the molten salt have an exponential relationship with temperature. Equations (1) and (2) are the fitting equations in the temperature range from 700 °C to 1000 °C, respectively.

$$\eta = 2.8204 \times 10^{-8} \exp\left(\frac{107747}{RT}\right) \quad (R^2=0.9962) \quad (1)$$

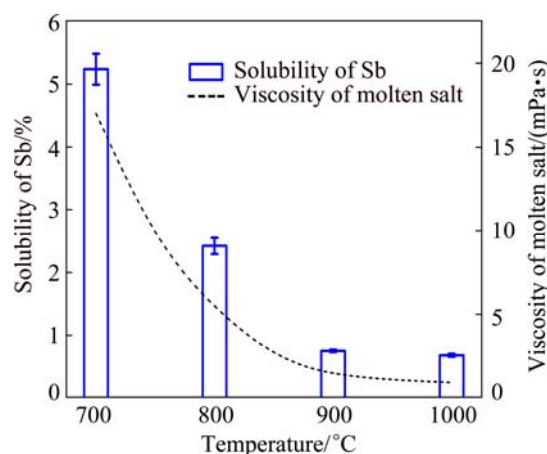


Fig. 2 Effect of temperature on solubility of Sb and viscosity of molten salt

$$S = 4.4770 \times 10^{-4} \exp\left(\frac{75838}{RT}\right) \quad (R^2=0.9885) \quad (2)$$

To further study the diffusion and distribution of Sb in molten $\text{Na}_2\text{CO}_3\text{-NaCl}$, surface scanning was performed for the top, middle and bottom regions of the cross-sections of the block samples calcined at different time and temperatures, as shown in Fig. 3. The surface scanning results indicate that the content of Sb dissolved in the bottom region is higher than that in the top region at 800 °C for 0.5 h of calculation. This finding is explained by the low diffusion rate of Sb and insufficient time elapsed. When the contact time is 3 h, the content of Sb in the whole section of salt sample remains nearly constant from the bottom to the surface. So the dissolution of Sb can be achieved in 3 h. When the calcination temperature was 1000 °C, the diffusion rate of Sb was high and the distribution of Sb was uniform after 3 h. But the quantity of Sb was small, because the viscosity of molten salt was small and mechanical loss of Sb was little.

To examine whether there is a phase change of the eutectic salts and Sb after the treatment at high temperature, X-ray diffraction was utilized to study the

supernatant salt and subjacent metal. Figure 4 shows the XRD patterns of the salt mixtures subjected to heat treatment from 700 °C to 1000 °C after 3 h and the metal specimen obtained after treatment at 800 °C after 3 h. By comparing the pattern with the standard card, all of the peaks in Fig. 4(a) were confirmed to arise from Na_2CO_3 (JCPDS card, No.37-0451) and NaCl (JCPDS card, No.05-0628). Furthermore, all of the peaks in Fig. 4(b) were identified as Sb (JCPDS card, No.35-0732). The results illustrate that molten salt and Sb did not react and the clarification of molten salt and antimony was excellent. The lack of detection of the Sb phase in the salt mixture might due to the insufficient content of Sb.

X-ray photoelectron spectroscopy was employed to examine the valence state of the elements in the sample calcined at 800 °C for 3 h. The survey spectrum of the sample is shown in Fig. 5. Sodium is present on the surface in the form of Na_2CO_3 and NaCl, with peaks at 1071.5 eV and 1072 eV, respectively. In the Cl 2p spectrum, the peaks are too weak to be detected. The peak at 531.1 eV of the O 1s spectrum can be attributed to carbonate. The two Sb 3d peaks can be attributed to Sb_2O_3 due to the oxidation of Sb on the surface.

Antimony is easily oxidized to generate Sb_2O_3

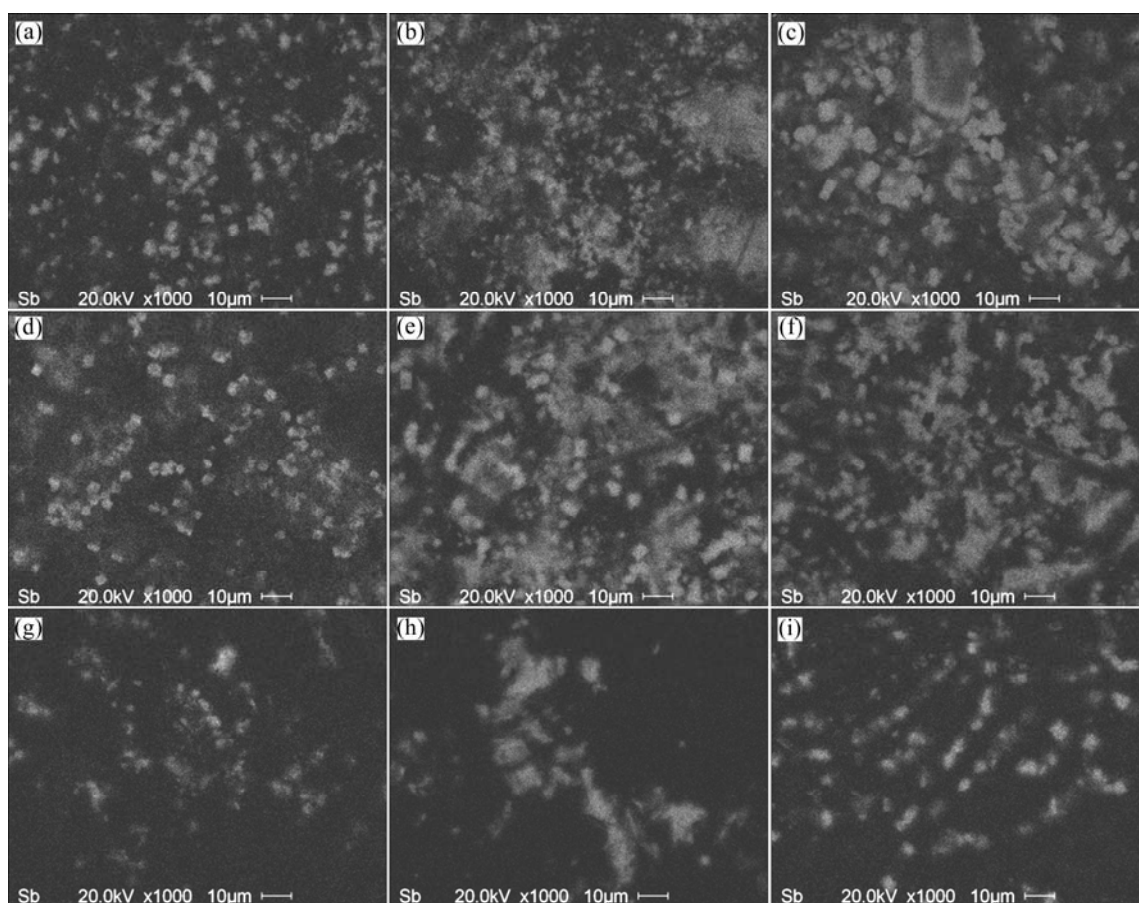


Fig. 3 Surface scanning results of Sb across block samples along diameter: Top (a), central (b) and bottom (c) regions of sample tested at 800 °C for 0.5 h; Top (d), central (e) and bottom (f) regions of sample tested at 800 °C for 3 h; Top (g), central (h) and bottom (i) regions of sample tested 1000 °C for 3 h

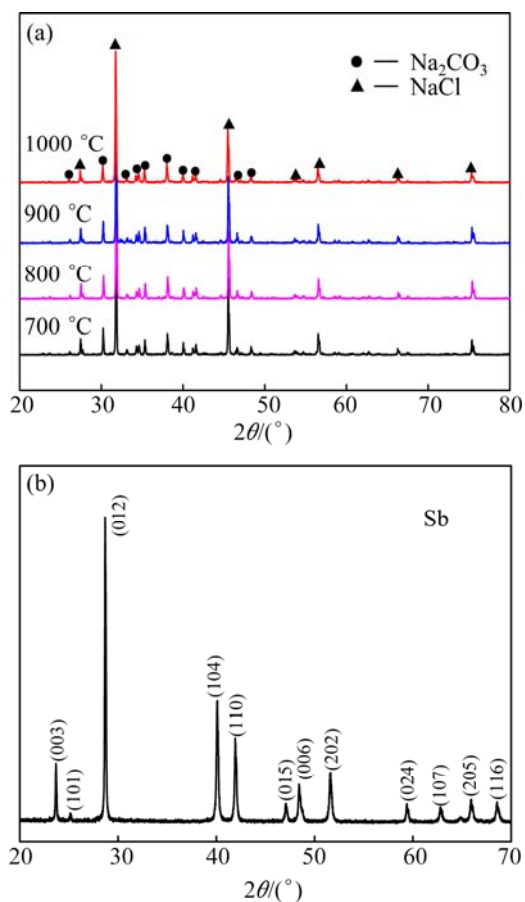


Fig. 4 XRD patterns of solid salts and metal after dissolution: (a) Solid salts; (b) Metal specimen

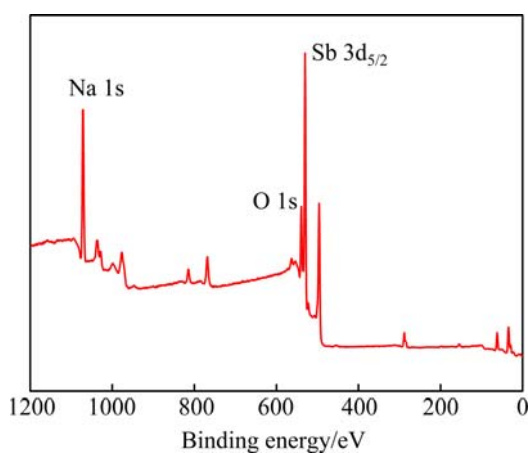


Fig. 5 XPS spectrum of eutectic mixture sample after dissolution

according to Reaction (3) [15,16]. Though the reaction was engaged under high purity argon, the p_{O_2} was still higher than 10^{-3} Pa. The change in the Gibbs free energy as a function of temperature and p_{O_2} calculated for the oxidation of Sb is shown in Fig. 6. The results showed that the oxidation of Sb can be spontaneous when the reaction temperatures were maintained between 500 °C and 1000 °C, as $\Delta G_T^\ominus < 0$. Although ΔG_T^\ominus increased as

the temperature and p_{O_2} decreased, the ΔG_T^\ominus value was still -199.45 kJ/mol at 1000 °C and $p_{O_2}=10^{-3}$ Pa. Therefore, the Sb on the surface of the molten salt was easily oxidized.

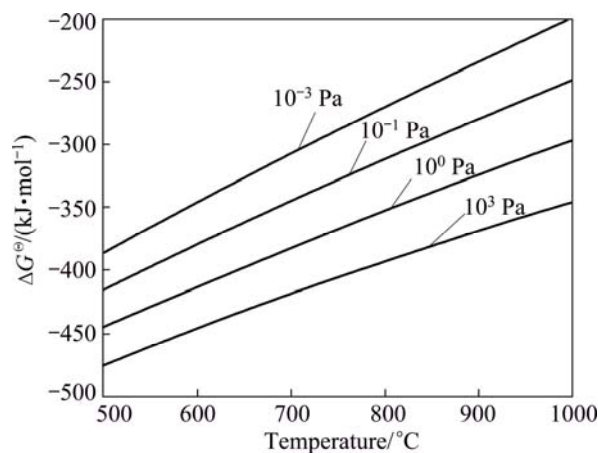


Fig. 6 ΔG^\ominus of oxidation reaction of Sb as function of temperature

The morphology of the sample obtained from heat preservation at 800 °C for 3 h was also studied. Figure 7 shows the SEM-BSE images and EDX spectra of the sample. The low-magnification image shows that the metal particles were randomly embedded in the salt (Fig. 7(a)), with no regular morphology. All of the particles were randomly embedded together across the solid granular powders. This phenomenon was observed clearly upon high-magnification, as shown in Fig. 7(b), and three particles combined tightly with an obvious interface. Figures 7(c), (d) and (e) show the EDX spectra of regions A, B and C in the SEM-BSE image. It could be conjectured from the mole fractions that phases B and C were NaCl and Na_2CO_3 , respectively. Phase A, the brightest point, was Sb grain. It can be seen from the pictures that most of the Sb particles were tightly embedded across the surface of the NaCl granular powders.

3.2 Effect of salt composition on solubility of Sb

The solubility of Sb and viscosity of molten salt at 900 °C are plotted against the salt content in Fig. 8. As the mole fraction of Na_2CO_3 increased from 0 to 0.4, the solubility of Sb decreased from 6.2719% to 0.764%, and the viscosity of molten salt increased from 8 to 2.7 mPa·s. This can be interpreted as follows. The solubility of Sb was determined by the viscosity of the molten salt, and the viscosity of the salt increased with increasing Na_2CO_3 contribution because Na_2CO_3 had a higher viscosity than NaCl. However, in the first stage ($n_{\text{Na}_2\text{CO}_3}/(n_{\text{Na}_2\text{CO}_3} + n_{\text{NaCl}}) < 0.4$), the melting point of the system will decrease with increasing Na_2CO_3 content;

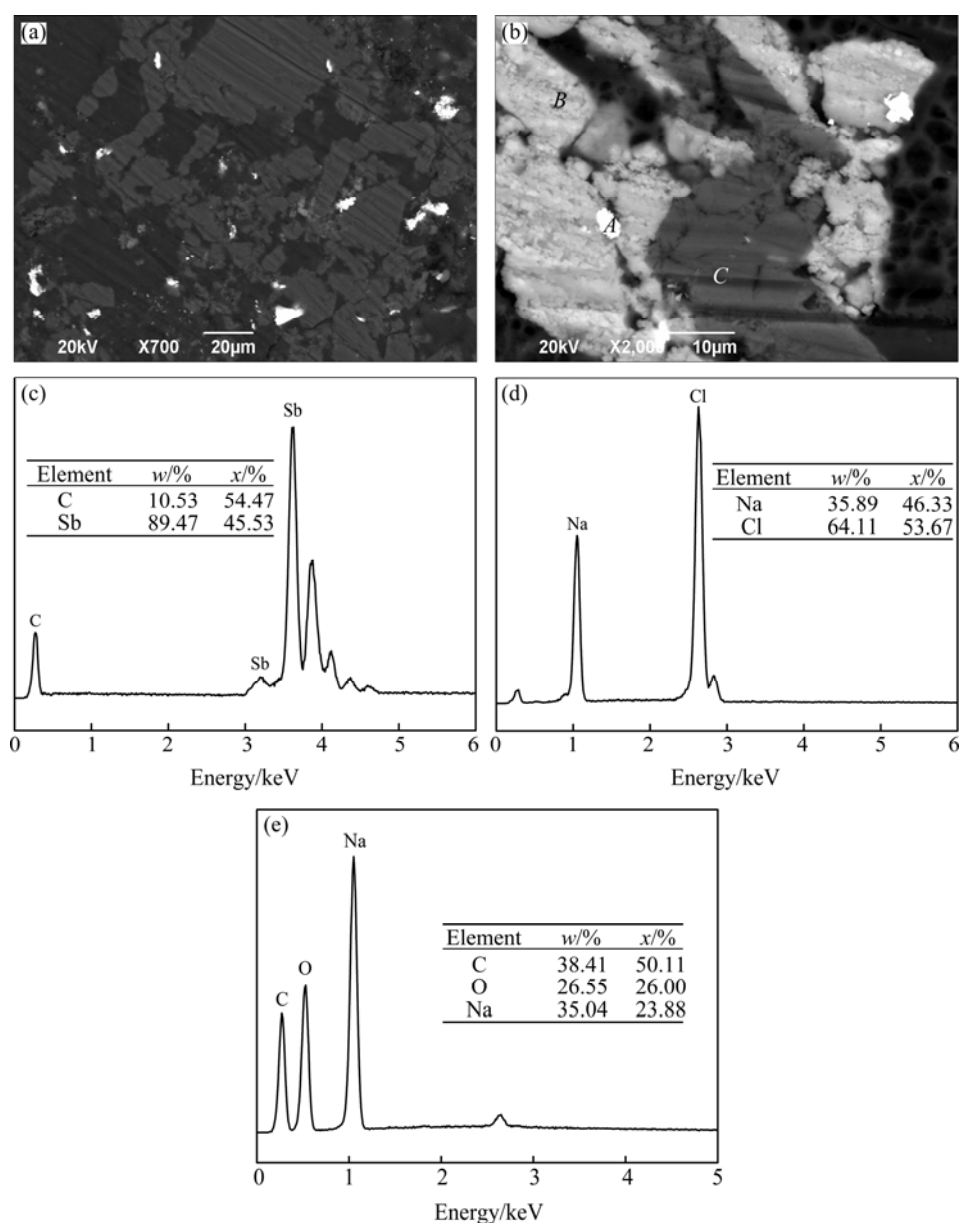


Fig. 7 SEM-BSE images and energy spectra of solid salt tested at 800 °C after 3 h: images at low magnification (a) and high magnification (b); EDX spectra of Region A (c), Region B (d) and Region C (e)

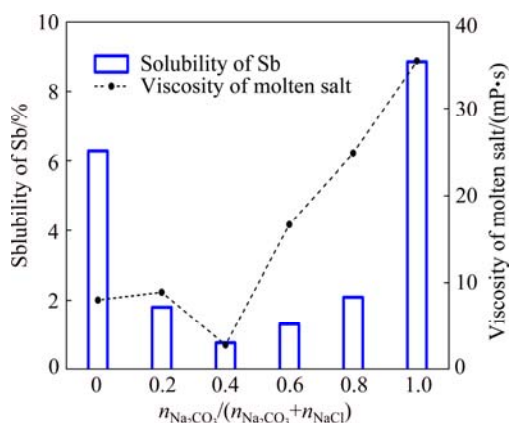


Fig. 8 Effect of NaCl content on viscosity of Na_2CO_3 -NaCl molten salt and solubility of Sb in this molten salt

thus, the viscosity of the system was the lowest at 0.4. Therefore, when the mole fraction of Na_2CO_3 was more than 0.4, both the solubility of Sb and the viscosity of the molten salt increased with increasing Na_2CO_3 content.

4 Conclusions

1) The dissolution equilibrium of Sb in molten salt can be achieved in 3 h depending on temperature, where high temperatures can accelerate the diffusion rate of Sb.

2) The viscosity of molten salt has a significant effect on the equilibrium solubility of Sb, and the amount of Sb dissolved in the melt decreases as the viscosity of molten salt decreases. Salt composition affects the

solubility of Sb by changing the melting point and viscosity of the molten system.

3) Metal Sb and molten salt do not react, and the elements do not change valence state with the exception of Sb, which is easily oxidized. All of the dissolved Sb particles embed together randomly across the solid granular powders.

References

- [1] CHEN G Z, FRAY D F, FARTHING T W. Direct electrochemical reduction of titanium dioxide to titanium in molten calcium chloride [J]. *Nature*, 2000, 407(6802): 361–634.
- [2] CHEN Zhao-yong, ZHU Wei, ZHU Hua-li, ZHANG Jian-li, LI Qi-feng. Electrochemical performances of LiFePO₄/C composites prepared by molten salt method [J]. *Transactions of Nonferrous Metals Society of China*, 2010, 20(5): 809–813.
- [3] ZHOU D, ZHAO C Y, TIAN Y. Review on thermal energy storage with phase change (PCMS) in building applications [J]. *Applied Energy*, 2012, 92(4): 593–605.
- [4] ZHAO C Y, WU Z G. Thermal property characterization of a low melting-temperature ternary nitrate salt mixture for thermal energy storage system [J]. *Solar Energy Materials and Solar Cells*, 2011, 95(12): 3341–3346.
- [5] FUJIWARA S, INABA M, TASAKA A. New molten salt systems for high temperature molten salt batteries: Ternary and quaternary molten salt systems based on LiF–LiCl, LiF–LiBr, and LiCl–LiBr [J]. *Journal of Power Sources*, 2011, 196(8): 4012–4018.
- [6] BAO Morigengaowa, WANG Zhao-wen, GAO Bing-liang, SHI Zhong-ning, HU Xian-wei, YU Jiang-yu. Electrical conductivity of NaF–AlF₃–CaF₂–Al₂O₃–ZrO₂ molten salts [J]. *Transactions of Nonferrous Metals Society of China*, 2013, 23(12): 3788–3792.
- [7] IWASAWA K, MAEDA M. Phase diagram study for the alkali metal-oxychloride system [J]. *Metallurgy and Materials Transaction B*, 2000, 31(4): 795–799.
- [8] QIAN Jian-gang, ZHAO Tian. Electrodeposition of Ir on platinum in NaCl–KCl molten salt [J]. *Transactions of Nonferrous Metals Society of China*, 2012, 22(11): 2855–2862.
- [9] JUN Y, KATSUNARI O, KOICHI A. Thermodynamic assessment of the KCl–K₂CO₃–NaCl–Na₂CO₃ system [J]. *CALPHAD*, 2007, 31(2): 155–163.
- [10] JUN Y, DAISUKE M, KOICHI A, YOUJI Y, HIROSHI Y. Strength of salt core composed of alkali carbonate and alkali chloride mixture made by casting technique [J]. *Materials Transaction*, 2007, 48(5): 1034–1041.
- [11] LV W Y, ZENG C L. Preparation of cohesive graphite films by electroreduction of CO₃²⁻ in molten Na₂CO₃–NaCl [J]. *Surface and Coatings Technology*, 2012, 206(219–220): 4287–4292.
- [12] YANG Jian-guang, HE De-wen, TANG Chao-bo, CHEN Yong-ming, SUN Ya-hui, TANG Mo-tang. Thermodynamics calculation and experimental study on separation of bismuth from a bismuth glance concentrate through a low-temperature molten salt smelting process [J]. *Metallurgy and Materials Transaction B*, 2011, 42(4): 730–737.
- [13] YANG Jian-guang, TANG Chao-bo, CHEN Yong-ming, TANG Mo-tang. Separation of antimony from a stibnite concentrate through a low-temperature smelting process to eliminate SO₂ emission [J]. *Metallurgy and Materials Transaction B*, 2011, 42(1): 30–37.
- [14] YE Long-gang, TANG Chao-bo, CHEN Yong-ming, YANG Sheng-hai, TANG Mo-tang. Thermal physical properties and stability of the eutectic composition in a Na₂CO₃–NaCl binary system [J]. *Thermochimica Acta*, 2014, 596(10): 14–20.
- [15] XU C H, SHI S Q, SURYA C, WOO C H. Synthesis of antimony oxide nano-particles by vapor transport and condensation [J]. *Journal of Materials Science*, 2007, 42(23): 9855–9858.
- [16] ZENG D W, CHEN X, JIANG R, XIE C S, ZHU B L, SONG W L. Thermal stability of Sb/Sb₂O₃ composition nanoparticles [J]. *Materials Chemistry and Physics*, 2006, 96(8): 454–458.

铋在 Na₂CO₃–NaCl 二元熔盐中的溶解度

陈永明¹, 叶龙刚¹, 唐朝波¹, 杨声海¹, 唐谟堂¹, 张文海^{1,2}

1. 中南大学 冶金与环境学院, 长沙 410083;

2. 中国瑞林工程技术有限公司, 南昌 330031

摘要: 研究了在 700–1000 °C 温度范围内金属铋在 Na₂CO₃–NaCl 二元熔盐中的溶解行为。结果表明, 金属铋的溶解平衡可以在 3 h 内完成, 同时铋的溶解量随熔体黏度的降低而减少。在 700、800、900 和 1000 °C 时铋的饱和溶解量分别为 5.42%、2.42%、0.75% 和 0.68%, 较高的温度和适量的 NaCl 含量可以降低铋的溶解量。不溶解的铋沉积于熔盐底部, 不与熔盐反应。溶解在熔盐表面的铋容易被氧化, 而溶解于熔盐中的铋以金属态的形式随机地分布于熔盐中, 形成夹杂。

关键词: 铋; 溶解度; 熔盐; 黏度

(Edited by Yun-bin HE)